

### 3 MICRON ICE-BAND ABSORPTION IN YOUNG STELLAR OBJECTS

JOHN A. GRAHAM<sup>1</sup>

Department of Terrestrial Magnetism, Carnegie Institution of Washington, Washington, DC 20015

Received 1997 April 2; accepted 1997 August 12

#### ABSTRACT

Profiles of the 3  $\mu\text{m}$  ice band with moderate spectral resolution ( $\lambda/\Delta\lambda = 1300$ ) are presented for four young stellar objects (YSOs). Of special interest is a comparison between those for the embedded HH 100 IR source and the FU Orionis star V346 Normae (V346 Nor) near HH 57, whose most recent outburst was in 1983. In the new spectra, there is no sign of the absorption feature at 2.97  $\mu\text{m}$  attributed by Graham & Chen in 1991 to ammonia ice. We now believe that this identification was spurious. The ice band in V346 Nor has a weaker long wavelength wing than that in HH 100 IR. It matches well a profile observed in the star Elias 13 that lies behind the Taurus dark cloud, and leads to the conclusion that the line of sight to V346 Nor passes through quiescent intracloud material rather than through the dense dust observed in emission at longer wavelengths. Fine structure in the ice-band wing, probably due to C–H stretch absorption, is detected at 3.47  $\mu\text{m}$  in the embedded objects HH 100 IR and [TS84] 13.1 in the Corona Australis cloud but not in V346 Nor. A second dip at 3.55  $\mu\text{m}$ , which is plausibly linked to CH<sub>3</sub>OH, is observed in HH 100 IR.

*Subject headings:* dust, extinction — ISM: individual (Corona Australis cloud) — stars: individual (V346 Normae) — stars: pre-main-sequence

#### 1. INTRODUCTION

Once a star is born within a parent molecular cloud, redistribution, dispersal, and processing of the remnant material rapidly ensue. Infall continues to build up the circumstellar disk, while the dynamical pressure of the circumstellar wind and the heating of the surroundings by the young star itself are primary agents in dispersal and processing. While it is easy to detect circumstellar gas in atomic form, study of the dust is more difficult. In some cases, we can infer dust properties from scattered light. However, the recent development of absorption-band spectroscopy in the infrared now allows us to detect energy transitions of matter in the solid state. Often in circumstellar dust, we are dealing with substances such as ices and organic molecules which are deposited in or grow upon the surfaces of dust grains. The fragility of these molecules predicates that they are very sensitive to changes in the physical conditions of their environment.

A strong absorption band at 3  $\mu\text{m}$  is seen in the spectra of young stellar objects which are, as yet, embedded within their parent clouds. The band is only observed in dense molecular clouds, not in the diffuse interstellar medium. There is good evidence, supported by laboratory experiment, that this feature is largely a result of amorphous ice that forms on dust grains which are protected from the harsh interstellar environment (Merrill, Russell, & Soifer 1976; Léger et al. 1979). Several years ago, Graham & Chen (1991) began a program to study the ice-band feature in dust around especially active young stars. One expects that the occasional intense outbursts that are observed in these objects might have a significant effect on the material left over from the star-forming process. The IR spectrometer on the Cerro Tololo Inter-American Observatory (CTIO) 4 m

telescope was used to obtain low-resolution profiles ( $\lambda/\Delta\lambda = 150$ ) of some young, barely visible stars as well as other, more deeply embedded, optically invisible, but strong IR point sources (Graham & Chen 1991; Chen & Graham 1993). Ice-band absorption was found in several objects. In some, peculiar absorption profiles were measured that suggested that a 2.97  $\mu\text{m}$  feature, possibly a result of ammonia ice, was present with a strength comparable to that of the water ice feature itself. This feature was not seen by others (e.g., Smith, Sellgren, & Brooke 1993; Whittet et al. 1996).

An opportunity came to reobserve a selection of objects with the now refurbished infrared spectrometer at CTIO in 1995 June. The instrument incorporated a  $256 \times 256$  pixel array with 30  $\mu\text{m}$  pixels making it possible to use a spectral resolution of 1300, 9 times the old value.

#### 2. NEW OBSERVATIONS

There were several limitations to this new series of observations. Because a high signal-noise ratio and high spectral resolution were essential to the observation procedure, only a few objects could be observed in the three-night run allocated. Included were three young stellar objects which cannot be seen directly in visible light and an FU Orionis object that became visible after an eruption in 1983. All had been previously observed by Graham & Chen (1991). The grating (75 lines  $\text{mm}^{-1}$ ) had a limited passband of 0.32  $\mu\text{m}$ , and three grating positions were required to bridge the spectral range 2.84–3.76  $\mu\text{m}$  with sufficient overlap to match each band. There was insufficient time to make simultaneous observations at 2  $\mu\text{m}$  (K band), which were needed to properly specify the continuum. A slit width of 1" was used throughout the run.

The observing procedure followed that of Smith, Sellgren, & Tokunaga (1989). Short integration times ranging from 1 to 3 s were used. At any one telescope setting, signal was accumulated for a total time of 1 minute. The telescope was then moved by a few arcseconds so that the star lay on a different part of the detector, and a second integration was

<sup>1</sup> Visiting Astronomer, Cerro Tololo Inter-American Observatory. CTIO is operated by AURA, Inc., under contract to the National Science Foundation.

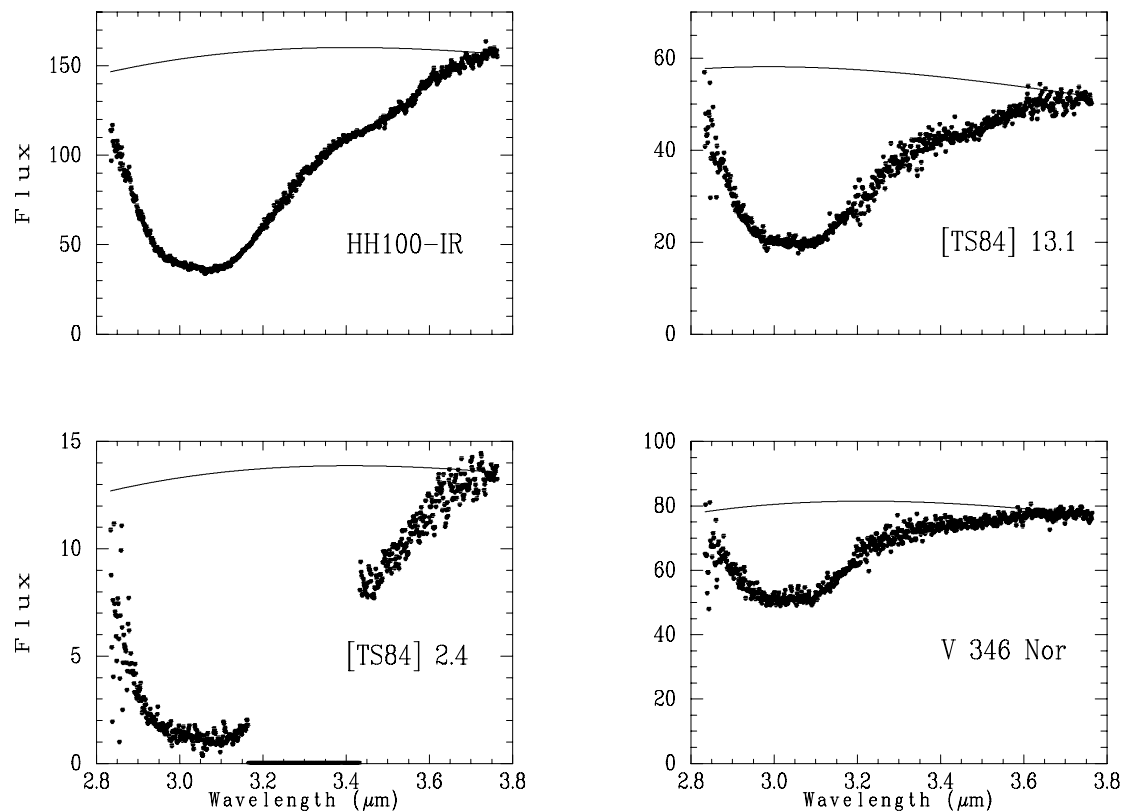


FIG. 1.—Intensity profiles of the 3 μm ice band. Flux is in units of 10<sup>-18</sup> W cm<sup>-2</sup> μm<sup>-1</sup>. Adopted black body energy distributions (see text) are shown as solid curves.

made. The sequence was repeated in reverse order. This comprised a single observation unit from which background subtraction, both thermal and sky, could be carried out effectively. A nearby bright reference star was chosen for atmospheric band removal.

An unsuccessful attempt was made to feed an Xe comparison beam into the optical path of the spectrometer. In default, the laboratory wavelength calibration of the grating tilt had to suffice, and was found adequate to within 0.01 μm. Much more serious was the discovery after the observations were made to find changing flexure within the spectrometer that produced differential displacements of up to 3 pixels (0.004 μm) in a spectrum on the array, even over telescope movements as small as 10°. If, as now seems likely, similar flexure occurred in the earlier series of low-resolution observations, it would have been very difficult to detect and would have led to serious atmospheric band contamination of the resulting spectra.

In the new series of observations, IRAF<sup>2</sup> routines were used to cross-correlate and shift the spectra before ratioing. Each ratioed spectrum was then multiplied by a blackbody spectrum whose temperature corresponded to that of the reference star. The intensity calibration was obtained by observing an Elias et al. (1982) standard star on each night and then using the Johnson (1966) zero-magnitude flux for the *L* band at 3.4 μm. These reduced spectra are shown as Figure 1.

Table 1 contains the program objects observed with coordinates (epoch 2000), and, on the right, the reference star parameters. The three wavelength bands observed were centered at 3.0, 3.3, and 3.6 μm. The spectra were mostly

<sup>2</sup> IRAF (Image Reduction and Analysis Facility) is distributed by the National Optical Astronomy Observatories, which are operated by the Association of Universities for Research in Astronomy, Inc., under contract with the National Science Foundation.

TABLE 1  
IR SOURCES OBSERVED AND REFERENCE STAR PARAMETERS

Object	R.A. (2000)	Decl. (2000)	Reference Star	Spectral Type	Blackbody Temperature
V346 Nor .....	16 32 32.2	−44 55 28	HR 6187	O5	40300
[TS84] 13.1 <sup>a</sup> .....	19 01 41.4	−36 58 31	HR 7211	A0 IV	9300
[TS84] 2.4 .....	19 01 47.8	−36 57 19	HR 7211	A0 IV	9300
HH 100 IR .....	19 01 50.6	−36 58 09	HR 7211	A0 IV	9300

NOTE.—Units of right ascension are hours, minutes, and seconds, and units of declination are degrees, arcminutes, and arcseconds.

<sup>a</sup> [TS84] refers to the IR source list published by Taylor & Storey (1984).

taken on different nights in each band so that a small ratio adjustment, using the overlap of  $0.02\text{--}0.03\text{ }\mu\text{m}$ , had to be made to merge adjoining spectra. This was typically 10%–15% and was principally because of the variable seeing and occasional high cirrus cloud during the observing run. [TS84] 2.4 was observed only at  $3.0$  and  $3.6\text{ }\mu\text{m}$ , so that no ratio adjustment could be made in this case.

### 3. THE 3 MICRON ICE FEATURE IN HH 100 IR

HH 100 IR was one of the first “protostellar” infrared sources to be identified (Strom, Strom, & Grasdalen 1974; Strom, Grasdalen, & Strom 1974). Although not seen directly in visible light, it illuminates an adjacent cone-shaped nebula which, like many of its type, shows perceptible morphological changes over a time base of several years (Graham 1993). This light, scattered from the deeply embedded source star, shows a chromospheric T Tauri-like spectrum (Cohen, Dopita, & Schwartz 1986). HH 100 IR was also one of the first in which absorption features produced by the surrounding dust were identified. Whittet & Blades (1980) found a feature at  $3.1\text{ }\mu\text{m}$  due to water ice. A strong solid CO feature due to silicates is seen at  $4.7\text{ }\mu\text{m}$  and at  $9.7\text{ }\mu\text{m}$  (Whittet et al. 1996). Through a strong outflowing wind, HH 100 IR excites several other Herbig-Haro (HH) objects in the vicinity (Hartigan & Graham 1987).

This source was the brightest object observed in this program. It is known to be variable (Axon et al. 1982; Reipurth & Wamsteker 1983), so there is the additional interest if the dust absorption also changes. Axon et al. (1982) discuss whether the IR fluctuations are due to vari-

able dust extinction or to changing infrared excess in the source. They conclude that both factors are effective. The best published ice-band profile is by Whittet et al. (1996). This was taken on 1988 April 24 with the UKIRT (United Kingdom Infrared Telescope) in Hawaii. It included a *K*-band measurement that provided a continuum reference, showing that the  $3\text{ }\mu\text{m}$  absorption extended to wavelengths shorter than  $2.8\text{ }\mu\text{m}$ .

To obtain an optical depth spectrum, one adopts an underlying continuum which is assumed, in this case, to be a blackbody spectrum. It is clear from the Whittet et al. (1996) profile that it would be incorrect simply to fit a blackbody spectrum to the  $2.8$  and  $3.8\text{ }\mu\text{m}$  points in the Figure 1 spectra. In the absence of *K*-band observations, it was decided instead to fix the  $3.8\text{ }\mu\text{m}$  point, and vary the blackbody temperature until a good fit could be obtained with the short-wavelength edge of the Whittet et al. (1996) spectrum. A result is shown in Figure 2 that produces remarkable agreement over the *whole* spectrum, including the maximum optical depth at  $\tau = 1.5$ . But, to obtain this agreement, a much higher blackbody temperature of  $850\text{ K}$  had to be assumed. The  $590\text{ K}$  blackbody temperature used by Whittet et al. (1996) would not have been sufficient to give a sensible profile. HH 100 IR was evidently unusually faint in 1988 April. Using the Johnson (1966) calibration, the Whittet et al. (1996) flux at *L* ( $3.4\text{ }\mu\text{m}$ ) corresponds to a magnitude of about 6.6. I observed the star shortly afterward (1988 August) at CTIO and measured *J:H:K:L:10*  $\mu\text{m}$  magnitudes of 15.44:11.04:7.70:5.01:0.86, respectively. The *L* flux of HH 100 IR in Figure 1 (1995 June) corre-

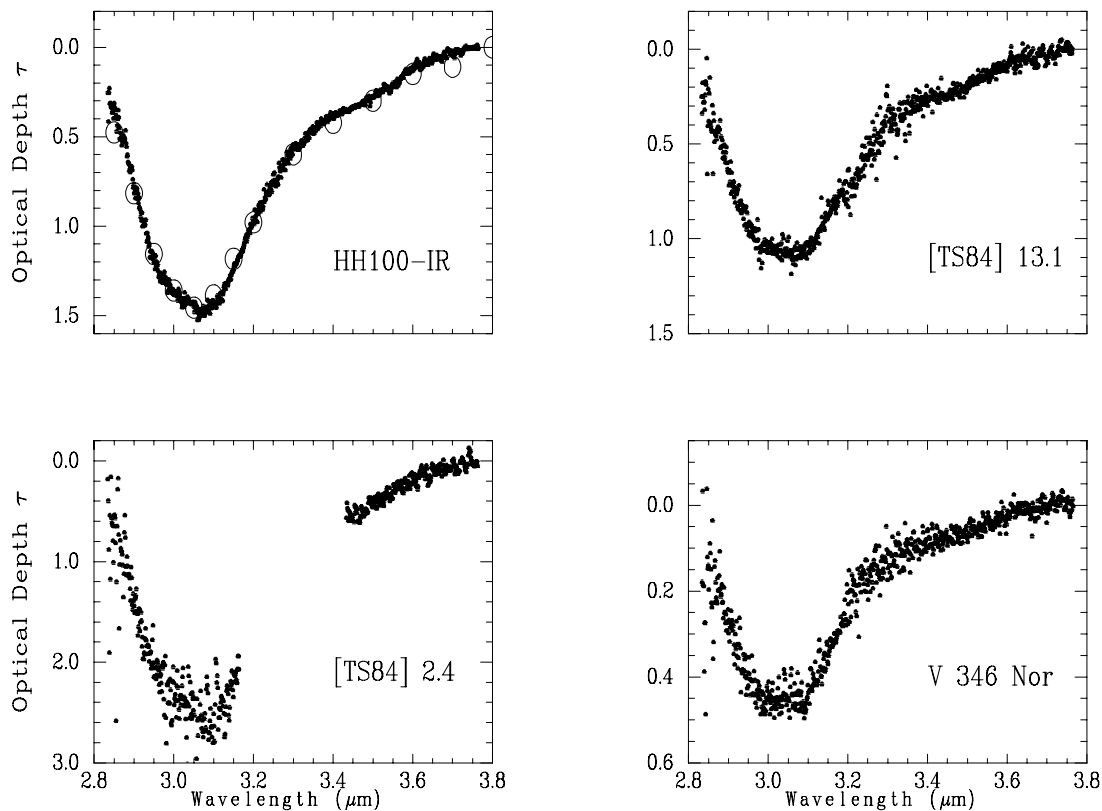


FIG. 2.—Optical depth  $\tau$  plotted against wavelength. Open symbols in the HH 100 IR plot are representative points from the profile published by Whittet et al. (1996).

sponds to an  $L$  magnitude of 4.6. Axon et al. (1982), Reipurth & Wamsteker (1983), and Molinari, Liseau, & Lorenzetti (1993) give tables that show a sampling of the variation at several wavelengths.  $L$  magnitudes as bright as 3.7 and as faint as 5.6 are included therein. Reipurth & Wamsteker (1983) find a range in apparent color temperatures of 650–950 K.

The constancy, on the other hand, of the optical depth spectrum of the ice feature shows that, at least for the icy dust grains, the absorption along the line of sight has not changed over a 7 yr baseline. The new spectrum supports a view that the photometric changes in HH 100 IR must be due entirely to a change in the intrinsic IR temperature (e.g., from heated dust close to the star) or else from variable absorption from some other type of dust particle.

#### 4. THE 3 MICRON FEATURE IN [TS84] 13.1 AND [TS84] 2.4

[TS84] 13.1 and [TS84] 2.4 are two other embedded objects in the CrA association. They were observed and cataloged by Taylor & Storey (1984) and Wilking, Taylor, & Storey (1986). Neither is directly visible, but both illuminate scattered light nebulae which appear enhanced in  $H\alpha$  images. The IR image of [TS84] 2.4 shows interesting structure in the  $H$  and  $K$  photometric bands (Chen & Graham 1993). It is evidently a double source. The object was also thought in our earlier work to have a strong ammonia ice band in its spectrum. The new high-resolution spectrum shows no such feature, and it appears that this identification was also due to an artifact caused by flexure in the spectrometer.

Optical depth profiles for these two objects are shown in Figure 2. Blackbody temperatures of 970 and 850 K were

used to define the continuum. These values were again chosen to give good agreement of the short-wavelength edges with the scaled profile for HH 100 IR. Maximum optical depths of 1.1 and 2.6 were found for [TS84] 13.1 and [TS84] 2.4, respectively. The [TS84] 2.4 value is imprecise because of the lack of the central-wavelength coverage and is uncertain to  $\pm 0.5$  in  $\tau$ . It is evident that ice absorption is heavy. Figure 3 shows all three of these spectra normalized to  $\tau = 1$  at  $3.0 \mu\text{m}$ . The points from the similarly normalized Whittet et al. (1996) HH 100 IR profile are superposed. The agreement is once again good and points to a basic similarity of the ice-grain absorbing material around each of the three sources.

#### 5. THE 3 MICRON FEATURE IN AN FU ORIONIS STAR

V346 Nor was first detected as an infrared source near the Herbig-Haro object HH 57 (Elias 1980; Reipurth & Wamsteker 1983). It is located near the eastern border of an elongated molecular cloud, Sandqvist 187 (Alvarez et al. 1986; Graham 1997). In 1983, Graham noticed a visible star that had not been seen before. In subsequent observations, it was shown to be a young pre-main-sequence star of the FU Orionis type (Graham & Frogel 1985; Reipurth 1985). Submillimeter observations have revealed large amounts of cool circumstellar dust (Weintraub et al. 1991; Reipurth et al. 1993). It is argued that so much dust would completely obscure the star unless it were distributed in a disklike configuration. One arcminute west, there is another embedded young star which is not directly visible, but which illuminates the small nebula Reipurth 13.

The ice-band feature in the V346 Nor spectrum, as shown in Figures 1 and 2, is weaker than the others reported here

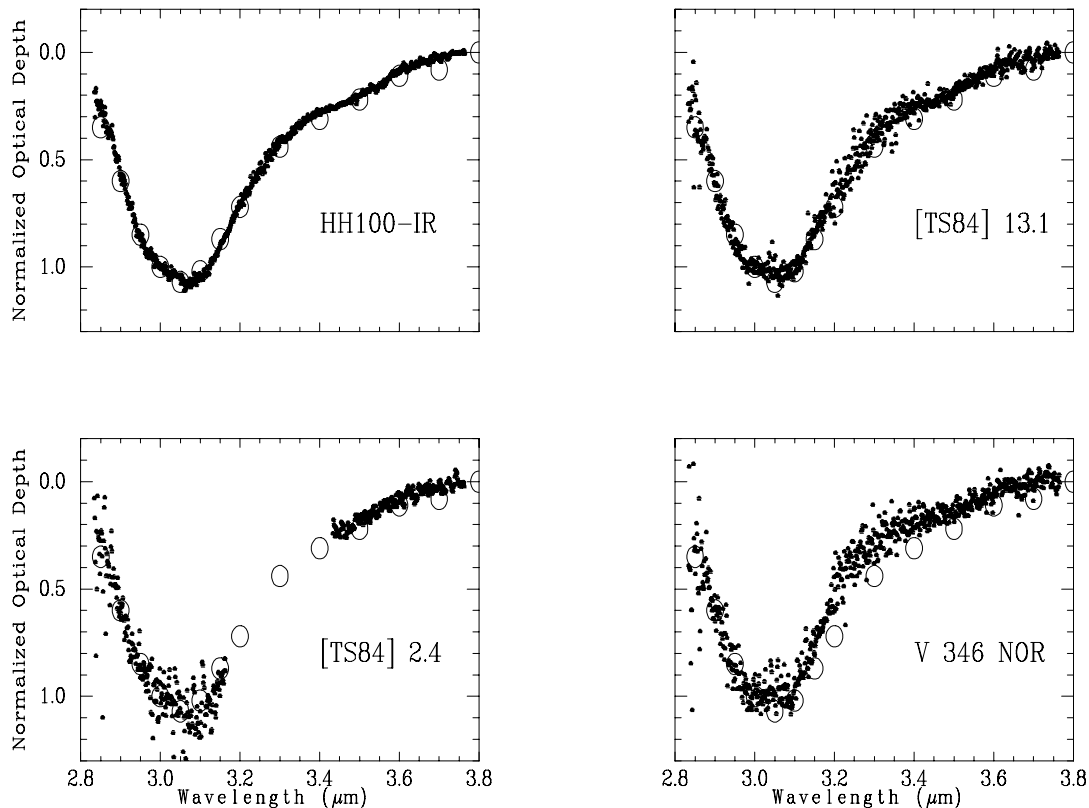


FIG. 3.—Optical depth profiles normalized to  $\tau = 1$  at  $3.0 \mu\text{m}$ . Open symbols are similarly normalized points from the Whittet et al. (1996) profile.

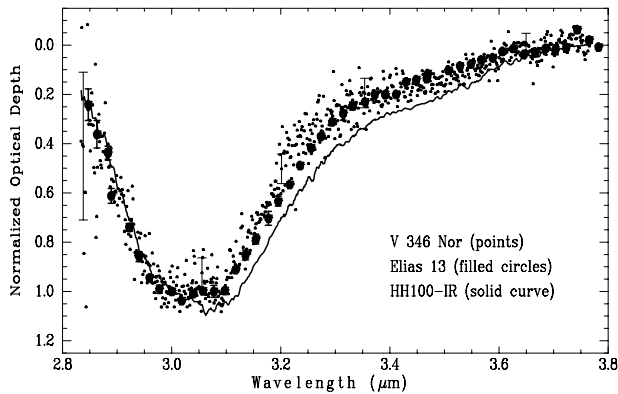


FIG. 4.—Comparison of normalized optical depth spectra for V346 Nor, Elias 13, and HH 100 IR. The Elias 13 data are from Smith, Sellgren, & Brooke (1993). Error bars characteristic of the individual V346 Nor and Elias 13 data points are shown.

( $\tau_{\max} = 0.46$ ). To obtain the most realistic continuum, the short-wavelength edge of the  $3\ \mu\text{m}$  absorption band was matched to that of a scaled spectrum of HH 100 IR. A temperature of 900 K fitted best. The profile was then normalized to  $\tau = 1$  at  $3.0\ \mu\text{m}$ . It is shown in Figure 3, along with the selection of points from a similarly scaled Whittet et al. (1996) spectrum. The long-wavelength wing is significantly more shallow than the absorption in the embedded CrA objects. In Figure 4 we compare the normalized profile with that of Elias 13, a K3 III star which lies *behind* the Taurus cloud (Elias 1978). The agreement is much better in this case. Smith, Sellgren, & Brooke (1993), who obtained these data, estimate a total absorption of about 12 mag in Elias 13. The full curve in Figure 4 reproduces the HH 100 IR absorption as plotted in Figure 2 but with smoothing over 9 pixels. Graham & Frogel's (1985) data indicate a total absorption of about 6 mag for V346 Nor. For Elias 13, Smith et al. (1993) investigate a series of grain models and find a good match to a population of silicate and graphite grains which have mantles whose thickness depends on the core radii.

It is perilous to generalize on an example of one star, but a basic difference between V346 Nor and the three CrA sources—HH 100 IR, [TS84] 13.1, and [TS84] 2.4—is that the optically invisible sources are still enveloped by cold dust remaining from the star-forming process, whereas the remnant material near V346 Nor is now confined to a disk inclined to the line of sight. From our viewpoint, only quiescent intracloud material is encountered as we observe the partially unveiled star. This is similar to the dust through which Elias 13 and other Taurus background stars are observed. Cloud core material still envelops and heavily obscures the CrA sources. It would be useful to examine other embedded stars that have recently attained visibility to see whether their ice band profiles have characteristics similar to that of V346 Nor. In this case, repeated FU Ori outbursts do not appear to be a relevant factor in accounting for the profile differences.

## 6. FINE STRUCTURE IN THE ICE-BAND WING

Weak absorption features characteristic of the C—H stretch vibrations are expected to be superposed on the long-wavelength wing of the ice-band absorption.

Allamandola et al. (1992) found well-resolved absorption bands at  $3.47$  and  $3.54\ \mu\text{m}$  in four embedded protostars. While the  $3.47\ \mu\text{m}$  feature could originate in several molecules, the  $3.54\ \mu\text{m}$  feature seems uniquely assignable to methanol,  $\text{CH}_3\text{OH}$  (Grim et al. 1991). Brooke, Sellgren, & Smith (1996) continued this work with further observations of nine embedded sources. Chiar, Adamson, & Whittet (1996) studied sources in and behind the Taurus dark cloud and made the first discovery of a very weak but significant  $3.47\ \mu\text{m}$  band in the background star Elias 16. These features were otherwise not seen when the line of sight passed through the quiescent cloud medium.

The  $3.47\ \mu\text{m}$  feature is detected in two of the spectra presented here, but not in the FU Orionis star. A quadratic was used to fit a continuum that contained and bridged the two windows  $3.35\text{--}3.40\ \mu\text{m}$  and  $3.60\text{--}3.65\ \mu\text{m}$ . This continuum was then subtracted from the optical depth spectra of HH 100 IR, [TS84] 13.1 and V346 Nor, and Elias 13. This led to the plots of  $\Delta\tau$  versus wavelength that are shown in Figure 5. Significant residuals are seen in the ice band profiles of HH 100 IR and [TS84] 13.1. Because of the incomplete spectral coverage, [TS84] 2.4 was not amenable to this treatment. The plotted points were then fitted with a fifth-degree polynomial and the resulting curves drawn in Figure 5. Neither V346 Nor nor Elias 13 show significant residuals from the continuum, but both HH 100 IR and [TS84] 13.1 show a depression in the polynomial fit at  $3.47\ \mu\text{m}$ . HH 100 IR also shows a feature at  $3.55\ \mu\text{m}$  which can be plausibly linked to the solid  $\text{CH}_3\text{OH}$  feature at  $3.54\ \mu\text{m}$ , observed by Allamandola et al. (1992) and Brooke et al. (1996). Each feature has  $\Delta\tau \approx 0.06$ , with respect to the broader ice wing. Following Allamandola et al. (1992), we find that the depth of the  $3.55\ \mu\text{m}$  feature corresponds to a number density ratio  $N(\text{CH}_3\text{OH})/N(\text{H}_2\text{O}) \approx 0.1$ , if attributed solely to  $\text{CH}_3\text{OH}$  absorption. Allamandola et al. (1992) remind us of the recurring discrepancy between this value determined at  $3.5\ \mu\text{m}$  and that determined from other features at longer wavelengths, possibly because of different light paths from the source. The absence of these absorption bands in the

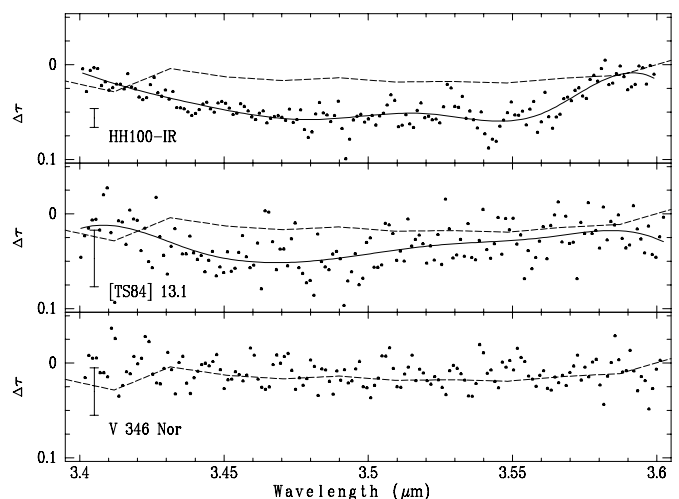


FIG. 5.—Weak absorption features in the long wavelength wings of the HH 100 IR and [TS84] 13.1 ice features. Fifth degree polynomial curves (solid) are fitted to residuals from an interpolated continuum (see text). Characteristic error bars are shown for individual points. The dashed lines join residuals determined in a similar way from the profile of Elias 13.

present spectrum of V346 Nor is additional evidence to suggest that we are viewing the star through quiescent intracloud dust rather than through circumstellar material close to the star.

### 7. CONCLUSIONS

The spectra presented in this paper were taken with a very specific aim—to investigate the reality of an absorption dip in the ice band at  $2.97\ \mu\text{m}$  which was attributed in earlier work to the presence of ammonia ice. New spectra have been obtained for four key objects with the highest resolution compatible with observing the full width of the water ice band. The principal results are as follows.

1. The feature reported earlier by Graham & Chen (1991) was an artifact probably produced by incomplete cancellation of atmospheric absorption features. The ultimate cause was most likely the flexure within the spectrograph.

2. New ice-band profiles with resolution 1300 ( $\lambda/\Delta\lambda$  over 2 pixels) covering  $2.8\text{--}3.8\ \mu\text{m}$  are presented for the embedded sources HH 100 IR, [TS84] 13.1, and [TS84] 2.4, in the Corona Australis association. These were taken in an observing run in 1995 June at CTIO. With some assumptions about the continuum, the HH 100 IR ice absorption optical depth profile remains unchanged in shape and in optical depth from when a similar observation was made 7 years earlier by Whittet et al. (1996). The earlier observation

was made when the IR source was faint, and the recent one when the IR source was bright. Thus, the variability of HH 100 IR is evidently not caused by changes in the obscuration by ice-covered dust grains.

3. The normalized optical depth profiles of all three embedded CrA sources are similar in shape.

4. HH 100 IR shows some fine structure in the long-wavelength wing. One band at  $3.47\ \mu\text{m}$  is probably due to C–H stretch absorption, and another at  $3.55\ \mu\text{m}$  may be due to  $\text{CH}_3\text{OH}$ . [TS84] 13.1 shows only the  $3.47\ \mu\text{m}$  band.

5. The spectrum of the FU Orionis star V346 Nor is both narrower and shallower than that of HH 100 IR. The difference does not appear to be the result of the FU Orionis outbursts. There is a very good match to the ice band spectrum observed in the star Elias 13 which lies behind the Taurus cloud. The line of sight to V346 Nor passes through material similar to the quiescent intracloud material in the Taurus cloud rather than through the dense cool dust observed at longer wavelengths.

I would like to express my gratitude to Doug Whittet for helpful comments on an earlier version of this paper. A referee is also to be thanked for a careful reading of the paper and for improvements to its content and style. This work was partially supported by NASA grant NAGW-4107 in the Origins of Solar Systems program.

### REFERENCES

- Allamandola, L. J., Sandford, S. A., Tielens, A. G. G. M., & Herbst, T. M. 1992, *ApJ*, 399, 134
- Alvarez, H., Bronfman, L., Cohen, R., Garay, G., Graham, J. A., & Thaddeus, P. 1986, *ApJ*, 300, 756
- Axon, D. J., Allen, D. A., Bailey, J., Hough, J. H., Ward, M. J., & Jameson, R. F. 1982, *MNRAS*, 200, 239
- Brooke, T. Y., Sellgren, K., & Smith, R. G. 1996, *ApJ*, 459, 209
- Chen, W. P., & Graham, J. A. 1993, *ApJ*, 409, 319
- Chiar, J. E., Adamson, A. J., & Whittet, D. C. B. 1996, *ApJ*, 472, 665
- Cohen, M., Dopita, M. A., & Schwartz, R. D. 1986, *ApJ*, 307, L21
- Elias, J. H. 1978, *ApJ*, 224, 857
- . 1980, *ApJ*, 241, 728
- Elias, J. H., Frogel, J. A., Mathews, K., & Neugebauer, G. 1982, *AJ*, 87, 1029
- Graham, J. A. 1993, *PASP*, 105, 561
- . 1997, *Carnegie Yearbook 95* (Washington, DC: Carnegie Inst. Washington), 50
- Graham, J. A., & Chen, W. P. 1991, *AJ*, 102, 1405
- Graham, J. A., & Frogel, J. A. 1985, *ApJ*, 289, 331
- Grim, R. J. A., Baas, F., Geballe, T. R., Greenberg, J. M., & Schutte, W. 1991, *A&A*, 243, 473
- Hartigan, P., & Graham, J. A. 1987, *AJ*, 93, 913
- Johnson, H. L. 1966, *ARA&A*, 4, 193
- Léger, A., Klein, J., de Cheveigne, S., Guinet, C., Defourneau, D., & Belin, M. 1979, *A&A*, 79, 256
- Merrill, K. M., Russell, R. W., & Soifer, B. T. 1976, *ApJ*, 207, 763
- Molinari, S., Liseau, R., & Lorenzetti, D. 1993, *A&AS*, 101, 59
- Reipurth, B. 1985, *A&A*, 143, 435
- Reipurth, B., Chini, R., Krügel, E., Kreysa, E., & Sievers, A. 1993, *A&A*, 273, 221
- Reipurth, B., & Wamsteker, W. 1983, *A&A*, 119, 14
- Smith, R. G., Sellgren, K., & Brooke, T. Y. 1993, *MNRAS*, 263, 749
- Smith, R. G., Sellgren, K., & Tokunaga, A. T. 1989, *ApJ*, 344, 413
- Strom, K. M., Strom, S. E., & Grasdalen, G. L. 1974, *ApJ*, 187, 83
- Strom, S. E., Grasdalen, G. L., & Strom, K. M. 1974, *ApJ*, 191, 111
- Taylor, K. N. R., & Storey, J. W. V. 1984, *MNRAS*, 209, 5P
- Weintraub, D. A., Sandell, G., & Duncan, W. 1991, *ApJ*, 382, 270
- Whittet, D. C. B., & Blades, J. C. 1980, *MNRAS*, 191, 309
- Whittet, D. C. B., et al. 1996, *ApJ*, 458, 363
- Wilking, B. A., Taylor, K. N. R., & Storey, J. W. V. 1986, *AJ*, 92, 103